Desalination and Water Treatment
www.deswater.com
doi: 10.1080/19443994.2015.1065767

57 (2016) 14708–14727
July

Taylor & Francis
Taylor & Francis Group

Batch and fixed bed column studies on removal of Orange G acid dye by a weak base functionalized polymer

Viorica Dulman[a], Simona-Maria Cucu-Man[a,*], Ion Bunia[b], Mihai Dumitras[a]

[a]*Faculty of Chemistry, Department of Chemistry, "Al. I. Cuza" University of Iasi, 11 Carol I Bd, 700506 Iasi, Romania, emails: dulmanv@yahoo.com (V. Dulman), sman@uaic.ro (S.-M. Cucu-Man), mihai.dumitras@uaic.ro (M. Dumitras)*
[b]*"P. Poni" Institute of Macromolecular Chemistry, 41A Grigore Ghica Voda Alley, 700487 Iasi, Romania, email: ibunia@icmpp.ro*

Received 27 January 2015; Accepted 18 June 2015

ABSTRACT

The performance of a weak base anion-exchange resin in removing Orange G dye from aqueous solutions in batch and column system was investigated. The adsorption capacity was found to depend on: pH, dye concentration, contact time, adsorbent dosage, electrolyte presence and temperature. The adsorption equilibrium is best described by the non-linear Langmuir isotherm model. At the optimum pH of 2, the maximum adsorption capacity was 1,076 and 1,218 mg g^{-1}, at 20 and 50°C, respectively. The adsorption kinetics could be described by the pseudo-second-order reaction model. The thermodynamic parameters indicated that adsorption is a spontaneous and endothermic process. FT-IR and SEM analyses provided additional information on adsorption mechanism and on morphological changes of the adsorbent. The breakthrough experimental results were processed by means of Thomas, Yoon–Nelson and Wolborska models. The reusability of the column was examined by conducting several cycles of adsorption and desorption (with 0.05 M NaOH).

Keywords: Adsorption; Orange G; Anion-exchange resin; Isotherms; Kinetics; Column

1. Introduction

Orange G (OG) (Acid Orange 10 or C.I. 16230) is a water-soluble acid azo dye with many applications. It is used for dyeing textiles (wool and silk), paper, leather, wood stain, colouring inks and copying pencils. Also, OG is used in histology in many staining formulations and is a pH indicator [1,2]. It is known that extended exposure to OG may lead to irritation of the respiratory and gastrointestinal tracts; it also affects anaerobic biomass in aqueous solutions [3]. Consequently, the efficient treatment of such industrial wastewaters is currently in real demand.

Various physical, chemical and biological treatments for dye removal, the acid dyes included, have been extensively investigated [4]. Among these methods, adsorption is considered to be one of the most effective and proven adequate technology, with high application potential in wastewater treatment using various natural or synthetic materials as adsorbents. The conditions established for the dyeing process make acid dyes ideal candidates for their removal by adsorption due to their structural characteristics [5,6].

Mesoporous-activated carbon of various origins was tested for OG [7–11]. The maximum adsorption capacity of these activated carbon adsorbents, from 9.129 to 236.07 mg g^{-1} [7,8], is still lower than that of some functionalized adsorbents.

*Corresponding author.

The use of ion-exchange resins for dye removal has either partially or wholly replaced traditional carbon treatments owing to good efficiency or low cost [12]. The ion-exchange resins have several advantages such as: the possibility of synthesizing certain materials with predetermined characteristics, their regeneration with economic benefits, no loss of adsorbent on regeneration, easy operation in dynamic conditions and recovery of dyes without chemical changes. Nevertheless, commercial ion-exchange systems have not been widely used for treatment of dye-containing effluents, probably due to the erroneous general opinion that ion exchangers cannot accommodate a wide range of dyes and perform poorly in the presence of other additives in wastewaters [13]. Subsequent results of various researchers have infirmed this view and suggested that ion exchangers in general could be effective adsorbents for dye removal. Of the commercial resins, the weak basic type (MP62, Bayer) showed the most favourable profile for reactive dyes: maximum loadings (230–900 mg g^{-1}) and complete regeneration [14]. The adsorption capacity of various synthesised polymeric adsorbents can be improved using monomers which have functional groups such as amino groups due to the specific interactions of these groups bound to the polymeric matrices with certain types of dyes [15].

The adsorption of dyes depends on the chemical structures of functional groups of the resin and on its porosity [14,16,17], but also on the structural properties of dyes [18–20]. In their works, Wawrzkiewicz and Hubicki [21–23] confirmed that removal of certain acid dyes depends on the matrices and the structure of polymers. Thus, for Acid Blue 29 adsorption on a strong basic anion exchanger with functional groups $–N^{+}(CH_3)_3$, the maximum monolayer capacity was 321.5 mg g^{-1} onto PuroliteA-520E (macroporous structure) and 83.3 mg g^{-1} on PuroliteA-520 (gel anion exchanger) against 30.2 mg g^{-1} on activated carbon. For the anionic textile dye Acid Green 9, the pyridine strong base anion-exchange resins have the highest adsorption values for the most hydrophilic structures, namely, pyridine resins with butyl, ethyl and methyl functional groups attached to the matrix. Their adsorption capacity was lower than the one obtained for the weak base anion-exchange resins (crosslinked acrylic copolymers functionalized with different amines) [24].

The adsorption characteristics of macroporous poly (glycidyl methacrylate-*co*-ethylene glycol dimethacrylate) (PGME) functionalized with diethylene triamine (PGME-deta) for OG are also superior to those of activated carbon. The dye was not retained by PGME, indicating that adsorption of this dye is specific through amino groups. It was shown that PGME-deta selectively adsorbs OG from binary solution with Bezaktiv Rot reactive dye [25].

Amino-functionalized acrylamide-maleic acid hydrogels are also highly swelling and have a high capacity for acid dye retention [26,27].

The functional poly(m-phenylenediamine) (PmPD) nanoparticles synthesized by Cu^{2+}-assisted method showed an adsorption capacity for OG of 387.6 mg g^{-1}, which is on average 200 mg g^{-1} more than that of the microparticles obtained by traditional chemical oxidative polymerization [28].

The dynamic dye adsorption through a commercial flatsheet ion-exchange membrane adsorbent was investigated and a strong correlation between fitted and experimental breakthrough curves for OG was obtained [29]. The study was extended to the separation of synthetic binary dye mixtures (OG, Eosin-B and Ponceau-S) [30].

In addition, various natural materials, inexpensive and easily available, have received during the last few years particular attention for the removal of dyes, but they have relatively low-binding capacities. Their chemical modification by functionalization with effective groups such as amino could improve their ability for the adsorption of dyes according to the nature of interactions between adsorbate and modified materials.

Thus, tetraethylenepentamine modified chitosan (TEPA-CS) is predicted to have better adsorption capacity for an anionic dye than EDA-CS because more imino groups are present in its chain [31]. Ethylenediamine-modified magnetic chitosan nanoparticles (EMCN) at 298 K and at pH 3.0 were determined to have a remarkable value of 1,017 mg g^{-1} for OG. Furthermore, the EMCN could be regenerated at pH 10.0 and could be reused [32].

The crosslinked starch-based materials, containing amine groups, exhibited interesting sorption properties for both the acid and reactive dyes. The interactions between anionic dyes and protonated tertiary amines play a major role in the sorption mechanism [18].

Ethylenediamine-modified starch [33], diethylenetriamine-modified native starch, diethylenetriamine-modified enzymatic hydrolysed starch [34] and dithiocarbamate-modified starch (DTCS) [35] are promising adsorbents for OG dye and other acid dyes. The lower adsorption capacity of a DTCS complex with Cu^{2+} for OG than for other acid dyes is attributed to the sulphonate groups located on the naphthalene ring [36,37].

Taking into account high water consumption in textile finishing, a suitable adsorption method would

be valuable for final treatment of colour effluent [14] and the ion exchange is an alternative to be considered. Several experimental results show that the wastewaters generated in polyamide dyeing with acid dyes can, after colour removal, be recycled in new preparation processes, such as scouring [38].

The aims of this work were to explore the potential use of a weak base anion-exchange resin for adsorption of OG acid dye and to establish the optimal adsorption conditions (initial solution pH, dye concentration, contact time between phases, adsorbent dosage and temperature). The isotherms, as well as the kinetic, thermodynamic and breakthrough curves for adsorption of OG on the ion-exchange resin were evaluated. The influence of various operational parameters such as bed height and flow rate on the breakthrough curves was examined.

2. Materials and methods

2.1. Dye

OG (synonyms: Acid Orange 10; 7-hydroxy-8-(phenylazo)-1,3-naphthalenedisulfonic acid disodium salt) with a pure dye content 95% was purchased from Aldrich and was used without any prior purification. According to the chemical structure (Fig. 1), the monoazo dye OG has the form of a disodium sulphonic acid salt, which determines its solubility in water. The OG molecule contains the azo chromophore group (responsible for the colour of the dye) and permanent solubilizing groups $–SO_3Na$ and –OH. It is known that the latter are responsible for the bonding between the fibre and the dye in dyeing process.

Stock solutions (1,000 and 2,000 mg L^{-1} pure dye) were prepared by dissolving accurately weighed quantity of dye (~95% purity) in double-distilled water.

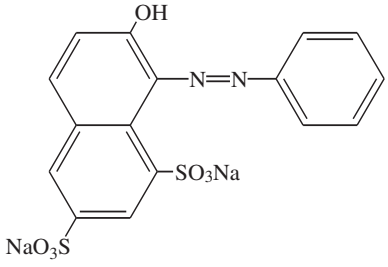

Fig. 1. Chemical structure of OG

2.2. Adsorbent preparation

The adsorbent (A2) used is a crosslinked acrylic copolymer based on divinyl benzene (DVB), ethyl acrylate (EA) and acrylonitrile (AN) functionalized with triethylenetetramine (TETA).

The copolymer was obtained using water suspension radical polymerization of DVB (2 wt.%), AN (20 wt.%) and EA (78 wt.%) in the presence of toluene as an inert component ($D = 0.4$). Ammonium salt of poly(styrene-co-maleic anhydride) was used as polymeric stabilizer in aqueous phase (0.5 wt.%). Benzoyl peroxide was used as initiator in all polymerization processes (1 wt.%). The aqueous/organic phase ratio was 3:1 (v/v). The reaction was allowed to proceed for 4 h at 65°C, 6 h at 75°C and 8 h at 85°C. Following polymerization, the copolymer beads were washed with warm water and then extracted with dichlorethane in a Soxhlet apparatus to remove traces of residual monomers, linear oligomers and diluent. Finally, they were vacuum dried at 50°C for 48 h.

The content of DVB units in the copolymer was assumed to be the same as the monomer content in feed. The samples (beads of 0.3–0.8 mm diameter) were characterized by uptake coefficients of methanol and toluene by centrifugation.

Aminolysis reactions were performed at 170–180°C with TETA, under reflux for 14 h in a glass round-bottomed flask equipped with stirrer, reflux condenser and thermometer. The copolymer:amine ratio was 1:5. After the reaction, the synthesized compounds were separated by filtration, washed with water and then regenerated with 4% NaOH aqueous solution. The aminolysis–hydrolysis reactions of DVB:AN:EA copolymer are given in Fig. 2.

The characteristics of the polymeric adsorbent are summarized in Table 1. As it can be observed, the

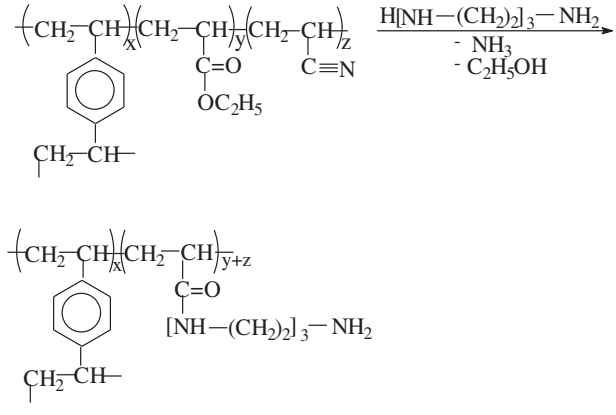

Fig. 2. Aminolysis-hydrolysis reactions of DVB:AN:EA copolymer.

Table 1
Characteristic data of A2 polymeric adsorbent

Characteristics	A2
Grade	Laboratory
Matrix	Cross-linked polyacrylate (DVB:EA:AN)
Active group	TETA
Chemical form	Free base
Physical form	Spherical beads
Crosslinking degree	2 wt.% DVB
Mean particle size, mm	0.3–0.8
Total exchange capacity	14.664 mEq g^{-1} (0.91 mEq mL^{-1})
pH range	1–14
Operational temperature	Until 80°C
Chemical stability	Good in acid and basic media

synthesized adsorbent has a high anion-exchange capacity. The polymer swells into a gel approximately 16 times its dry volume after equilibration with water for 24 h.

2.3. Batch adsorption and column experiments

The effect of certain parameters on the OG adsorption onto the A2 polymer was studied in batch mode. All kinetic and equilibrium experiments were carried out with a quantity of adsorbent introduced into a solution of known concentration of dye and varying initial pH, contact time between dye and polymer, adsorbent dose, initial dye concentration and temperature.

The initial pH was adjusted from 1.0 to 7.0 by addition of diluted HCl or NaOH. To investigate the effect of the contact time on OG removal, 0.25 g A2 polymer were inserted in 100 mL aqueous dye solution with initial concentration between 25 and 750 mg L^{-1}, and continuously stirred at a constant temperature of 25°C. Samples were withdrawn at appropriate time intervals and the residual dye concentration was measured spectrophotometrically on an UV-1700 Pharma Spec-spectrophotometer (Shimadzu) at λ = 485 nm.

Equilibrium studies were performed at the optimum pH 2, after a contact time between phases of 20 h (sufficient for the equilibrium to be reached), at three temperatures in the range of 298–323 K for various dye concentrations (from 25 to 2,000 mg L^{-1}). Dye equilibrium concentration was determined as mentioned above.

The effect of adsorbent dosage on the dye removal and polymer adsorption capacity was examined by varying the amount of adsorbent from 0.02 to 0.25 g/14 mL (1.43–17.86 g L^{-1}) at a constant initial dye concentration of 284 mg L^{-1}.

The influence of Na_2SO_4 on OG dye adsorption has been tested in the following conditions: dye concentration of 400 mg L^{-1}, pH 2, 2.5 g L^{-1} adsorbent, contact time 20 h and temperature 20°C.

The amount of adsorbed dye at time t, q_t (mg g^{-1}) and at equilibrium, q_e (mg g^{-1}) was calculated by (Eq. (1)):

$$q_t = \frac{(C_0 - C_t)V}{w} \tag{1}$$

where q_t is the amount of dye adsorbed at time t (mg g^{-1}); C_0 is the initial dye concentration in solution (mg L^{-1}); C_t is the concentration of dye solution at time t (mg L^{-1}); V is the volume of dye solution (L); and w is the mass of adsorbent used (g).

All the results were related to the mass of dry adsorbent (105°C). For t sufficiently large for the equilibrium to be established, Eq. (1) is used to calculate the amount of dye adsorbed at equilibrium (q_e). The percentage removal R (%) was obtained by (Eq. (2)):

$$R\ (\%) = \frac{(C_0 - C_e)}{C_0} \cdot 100 \tag{2}$$

where C_e is dye concentration in solution at equilibrium (mg L^{-1}).

In the column adsorption experiments, a known quantity of A2 resin (0.05–0.15 g) was transferred into a 25 mL beaker where 20 mL of double-distilled water was added. The adsorbent was kept for swelling at room temperature overnight. A glass column (9 mm internal diameter and 7 cm height) was packed with swollen polymer. The dye solution of 750 mg L^{-1} (pH

2) was allowed to feed through the polymer in a downflow mode. The desired flow rate (34.2, 52.2, 67.8 mL h^{-1}) was maintained using a peristaltic pump. Effluent samples were taken from the bottom of the column at fixed time intervals using a sample collector. The dye concentration was spectrophotometrically determined.

The dye desorption from the polymer loaded with OG in basic medium was tested in dynamic conditions. Samples of 0.05 g polymer with 2.5 mg adsorbed dye were treated with 35 mL of NaOH solution with concentrations of 0.01, 0.05, 0.1 and 0.5 mol L^{-1}, at a flow rate of 0.5 mL min^{-1}. Successive samples of 2 mL were collected to determine the concentration of the eluted dye.

2.4. Polymer characterization before and after dye adsorption

Scanning electron microscopy (SEM) analysis was carried out on the ion exchanger functionalized polymer to study its surface texture before and after OG dye adsorption. The polymer samples were analysed with a LEITZ microscope, using an acceleration voltage of 10 kV. The samples were fixed with colloidal silver on an aluminium support and then covered with a thin gold layer.

The FT-IR spectra for adsorbent before and after dye adsorption were recorded on a Vertex 70 Bruker FT-IR spectrometer, in the 4,000–450 cm^{-1} region in KBr pellets.

DTA and thermogravimetric analysis of the functionalized polymer (A2) and of the material obtained after dye adsorption (A2-OG) were carried out on a Diamond Pyris TG-DTA (Perkin-Elmer) system. The measurements were performed under nitrogen, with a heating rate of 10 K min^{-1}, sample mass 4 mg, using freshly calcinated Al_2O_3 as reference.

3. Results and discussion

3.1. Effect of pH

In an adsorption process, the initial pH of dye solution (pH_i) is a very important factor because it significantly influences the chemistry of both adsorbent and dye molecules. The pH_i of solution affects firstly the charge of the adsorbent surface, since the acrylic polymer was functionalized with a polyamine (TETA) and the protonation of amine groups leads to a large number of positively charged sites. Secondly, dye ionization is pH-dependent. The OG acid dye is a disodium salt of the organic sulphonic acid with general formula of R-$(SO_3)_2Na_2$ that in aqueous solution dissociates in coloured sulphonate anions R-$(SO_3)_2^{2-}$.

The pH_i effect in the range of 1.0–7.0 on the A2 adsorption capacity is illustrated in Fig. 3. It shows that the amount adsorbed at equilibrium is pH dependent. One can notice that a total removal of OG dye occurs at pH 2, value considered to be optimum in all subsequent experiments. The decrease in percentage removal at pH 1 (84.5%) may be due to the decrease in dye dissociation which leads to a lower concentration of the anionic dye species available to interact with the active sites of adsorbent. One can also see that dye adsorption decreased from 100 to 70%, respectively, with increasing pH from 2 to 7, due to a considerable decrease of the positive surface charge density. Donia et al. [19] reported that OG dye adsorption on monoamine-modified silica particles is optimum at pH 3 and the adsorption capacity dependence on pH is similar.

After dye adsorption, the final pH values of the solution (pH_f) increased slightly for pH_i of 1–2 and some more for pH_i values in the range 3–6 (Fig. 3). This finding can be explained by protonation of adsorbent amine groups. At a lower pH, more protons will be available that produce a smaller change of pH_f as compared to the weak acidic solution. Around pH 7, the protonation of amine groups is low due to low concentration of free H_3O^+ and consequently, the increase of the pH will be lower.

As the results reflect the pH dependence of the OG dye removal with the A2 polymer, it is obvious that adsorption process mainly occurs through electrostatic interactions between the sulphonate anionic groups

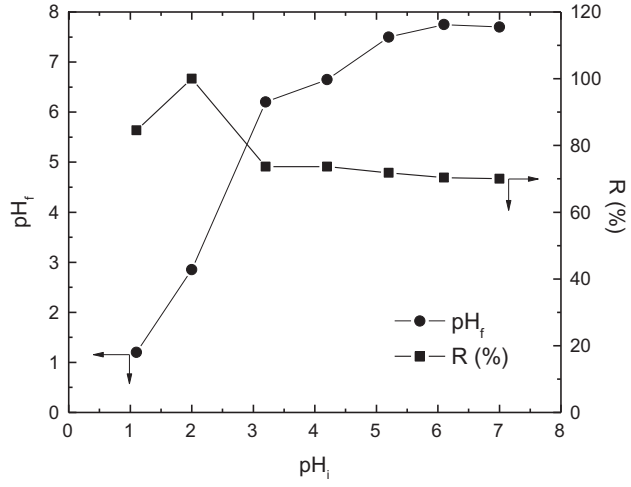

Fig. 3. Effect of initial pH on OG dye adsorption and variation of the pH after dye removal (w = 0.05 g; V = 20 mL; C_0 = 25 mg L^{-1}; 25°C; 20 h).

that belong to the dye and the positively charged protonated amino groups on the surface of adsorbent. The equilibrium in Fig. 4 illustrates dye interaction with primary amine groups of polymer.

The reaction of other two acid dyes with polymers was also described as an ionic-exchange mechanism. The adsorption capacity of a hydrogel with amino group incorporated (H-TETA polymer) for Indigo carmine increased with decreasing pH and it was maximum at pH 3 [27]. The same behaviour was observed for the adsorption of the Acid Blue 74 dye on the weak base anion exchanger Amberlite FPA51 [23].

3.2. Effect of the contact time. Kinetic modelling of the dye adsorption

Fig. 5 shows the influence of the contact time on the adsorption of OG dye on A2 polymer from solutions with initial concentration in the range of 25–750 mg L^{-1}. The shape of the curves is smooth and continuous leading to equilibrium. It is also evident that for each dye concentration a higher rate of adsorption is attained at the beginning and then it tends to reach a plateau. At low initial concentrations (25 and 50 mg L^{-1}), approximately 61–62% of the dye is removed in 5 min and 100% in 20–30 min.

At higher concentrations (500 and 750 mg L^{-1}), around 67% dye was rapidly adsorbed, in 10 and 20 min, respectively, followed by a slower process. The equilibrium was attained within 180 min when the dye was quantitatively removed. The q_t value increases from 10.17 to 371.8 mg g^{-1} with the initial concentration of dye increasing from 25 to 750 mg L^{-1}.

The uptake of the anionic dye is faster during the first minutes when most of the functional groups on

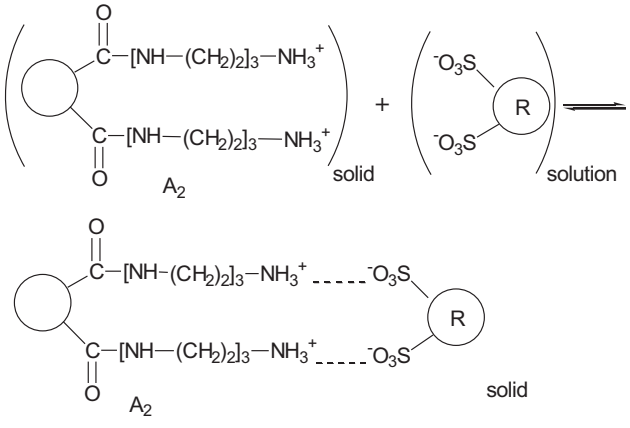

Fig. 4. Interaction of dye with primary amine groups of polymer.

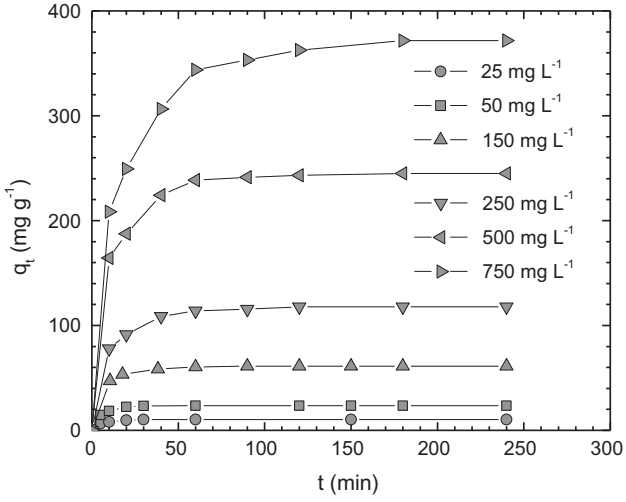

Fig. 5. Effect of initial concentration and contact time on adsorption of OG from dye solution (w = 0.25 g; V = 100 mL; 25°C).

the surface of adsorbent are available. Approaching equilibrium, the remaining surface sites may be difficult to occupy due to sterical hindrance. Thus, the retention becomes slower for high dye concentrations as the surface adsorption sites are exhausted and a process of gradual diffusion in pores, where additional active sites are available, takes over the adsorption kinetics before the equilibrium is attained [39].

The kinetic models (pseudo-first-order, pseudo-second-order and Elovich) and intraparticle diffusion model presented in Table 2 have been applied to A2 polymer–OG dye system.

Ho et al. [40] pointed out that the distinction between kinetic and diffusion adsorption is often difficult to define. Roughly speaking, it can be assessed that when equilibrium is achieved within three hours, the process is usually kinetically controlled and if it takes more than 24 h, it is diffusion controlled. Either or both kinetic and diffusion processes may be rate controlling within a three to twenty-four hours period.

Kinetic parameters of pseudo-first-order, pseudo-second-order and Elovich models for OG adsorption on A2 for dye concentration in the range of 25–750 mg L^{-1} were calculated from the plots according to linear equations and are given in Table 3.

It was found (Table 3) that application of pseudo-second-order kinetics provides better correlation of the experimental data than the pseudo-first-order model. In addition, there is much difference between the equilibrium adsorption capacities determined from the pseudo-first-order kinetic model and those experimentally determined.

Table 2
Linear equations of the applied kinetic models

Kinetic model	Linear equation	Plot	Reference
Pseudo-first-order	$\log(q_e - q_t) = \log q_e - \frac{k_1}{2.303}t$	$\log(q_e - q_t)$ vs. t	[40]
Pseudo-second-order	$\frac{t}{q_t} = \frac{1}{k_2 q_e^2} + \frac{1}{q_e}t$	$\frac{t}{q_t}$ vs. t	[40]
Elovich	$q_t = \frac{1}{\beta}\ln(\alpha\beta) + \frac{1}{\beta}\ln t$	q_t vs. $\ln t$	[41]
Intraparticle diffusion	$q_t = k_{id}\cdot t^{0.5} + I$	q_t vs. $t^{0.5}$	[42]

Elovich model is based on a kinetic principle assuming that the number of adsorption sites increases exponentially with adsorption, which implies a multilayer adsorption. The Elovich parameters could be computed from the plots of q_t vs. ln t. The calculated data indicate that the values of α, Elovich initial adsorption rate (mg g^{-1} min^{-1}), and β, Elovich constant (g mg^{-1}), depend on the initial dye concentration. The obtained correlation coefficients are between 0.9003 and 0.9884. Thus, is obvious that the pseudo-second-order model describes more appropriately the investigated system.

The diffusion mechanism can be identified by using the intraparticle diffusion model proposed by Weber and Morris (Table 2). This model is considered adequate for describing the adsorption when, by plotting q_t vs. $t^{0.5}$, a straight line passing through the origin is obtained [40]. The plots that do not pass through the origin indicate a certain degree of boundary layer control and also that the intraparticle diffusion is not the only rate-limiting step. In this case, the adsorption process is complex and several kinetic models that operate simultaneously can be used.

The rate constants of intraparticle diffusion (k_{id}) were obtained from the linear part of the plots q_t vs. $t^{0.5}$ for different OG dye concentrations (Table 4). The k_{id1} values increase from 1.199 to 29.691 mg g^{-1} min$^{-0.5}$ with the increase in dye concentration from 25 to 750 mg L^{-1}. This is presumably due to a greater driving force with increasing C_0 that enhances the diffusion in pores of the gel. Similar results were reported for adsorption of Acid Blue 161 on certain biosorbents [6]. The R^2 values for the intraparticle diffusion model were between 0.9406 and 0.9987. For the initial dye concentrations of 500 and 750 mg L^{-1}, two separate segments were found in the plot, namely, the first linear segment has the same meaning with the one mentioned above (rate constant k_{id1}). The second linear segment can be attributed to advanced diffusion to the least accessible sites of adsorption of the gel pores with rate constant k_{id2} of 1.128 and 4.988 mg g^{-1} min$^{-0.5}$, for the two concentrations, respectively. In the first stages, rapid adsorption kinetics take place in the gel pores, as indicated by the high k_{id1} as compared with low k_{id2} values, when migration of adsorbate is very slow. In the case of OG removal by adsorption onto bagasse fly ash the constant values obtained were: k_{id1} 0.565 mg g^{-1} min$^{-0.5}$ and k_{id2} 0.0292 mg g^{-1} min$^{-0.5}$ [43].

As the plots did not have a zero intercept it may be concluded that liquid film diffusion and intraparticle diffusion were concurrently operating during interaction of OG dye with surface adsorption onto the polymer [41]. The values of the intercept increase from 3.9 to 115.9 mg g^{-1} for higher concentrations, indicating a greater contribution of the surface adsorption in the rate-controlling step.

3.3. Effect of initial dye concentration. Adsorption isotherms

Initial dye concentration is an important factor on which the amount of dye that can be retained from a solution onto an adsorbent depends. The adsorption isotherms are useful for characterizing any adsorption system that reached an equilibrium state. An adsorption isotherm expresses the relationship between the mass of species adsorbed at constant temperature per mass unit of the adsorbent (q_e) and the species concentration left in the solution (C_e). The shape of the obtained isotherm gives information about the nature of the adsorbent-adsorbate interactions.

The adsorption isotherms for the A2 adsorbent–OG dye system (Fig. 6) show that there is an increase in the amount of dye adsorbed when the initial dye concentration (C_0) was raised in the wide range from 25 to 2,000 mg L^{-1}. The same trend is observed for the three temperatures tested, namely 298, 308 and 323 K. The isotherms have a sharp part at low dye concentrations from 25 to 150 mg L^{-1} (when the dye retention is 100%) indicating that the dye molecules have access to an excess of sites available for adsorption. With increasing initial dye concentration, the number of

Table 3
Kinetic parameters for OG adsorption on A2 at different initial dye concentrations

C_0 (mg L^{-1})	q_e (mg g^{-1})	Pseudo-first-order			Pseudo-second-order			Elovich		
		q_{ec} (mg g^{-1})	k_1 (min^{-1})	R^2	q_{ec} (mg g^{-1})	$k_2 \times 10^4$ (g mg^{-1} min^{-1})	h (mg g^{-1} min^{-1})	R^2	α (mg g^{-1} min^{-1})	β (g mg^{-1})	R^2
25	10.2	8.1	0.1400	0.9975	10.3	589.9	6.22	0.9998	7.99	0.4515	0.9884
50	23.6	16.5	0.1225	0.9947	23.9	233.2	13.28	0.9995	46.84	0.2637	0.9003
150	61.2	25.0	0.0573	0.9992	64.5	12.44	6.95	0.9978	82.16	0.1528	0.9621
250	117.9	49.2	0.0364	0.9541	120.5	17.40	25.25	0.9998	211.12	0.0602	0.9508
500	244.9	113.6	0.0352	0.9565	250.0	8.42	52.63	0.9998	466.31	0.0293	0.9456
750	371.8	490.2	0.0263	0.9751	384.6	2.80	41.49	0.9997	161.31	0.0152	0.9772

Notes: q_e experimental.
q_{ec} calculated (mg g^{-1}).

unoccupied active sites at equilibrium decreases with a small increase in q_e values that tend to reach saturation concomitantly with substantial decrease in C_e. In the concentration range tested, C_e decreased with increasing temperature. For example, at the highest initial dye concentration, the C_e value varies from 165 to 14 mg L^{-1} with temperature increasing from 298 to 323 K. H-type isotherms at different temperatures suggest a high affinity for the surface assuming involvement of chemical forces rather than physical attraction [44]. The experimental data for OG adsorption on A2 were examined by several adsorption isotherm models (in non-linear form): Langmuir, Freundlich, Redlich–Peterson and Sips (corresponding equations given in Table 5). Model parameters and R^2 values were obtained by non-linear regression, as summarized in Table 6.

The Langmuir isotherm is characteristic for a monolayer adsorption on a surface containing a limited number of identical sites [45].

The Langmuir equilibrium constant K_L (L g^{-1}) was calculated as (Eq. (3)):

$$K_L = q_m \cdot b \tag{3}$$

Generally, the values of K_L show the adsorbent affinity for the adsorbate, related to the free energy of adsorption. The dimensionless constant R_L (separation factor) provides information about whether the adsorption process is spontaneous or non-spontaneous. It can be computed as follows (Eq. (4)):

$$R_L = \frac{1}{1 + bC_0} \tag{4}$$

The value of R_L indicates an irreversible adsorption process when $R_L = 0$; favourable when $0 < R_L < 1$; linear when $R_L = 1$; and unfavourable when $R_L > 1$.

For the polymer A2-OG dye system the values of K_L rise strongly from 40.9 to 269.2 L g^{-1} in the range of temperature between 298 and 323 K. The highest q_m value was found to be 1,218 mg g^{-1} at 323 K, compared to 1,076 mg g^{-1}at 298 K. These results indicate that in aqueous solution at pH 2 the adsorbent shows high affinity for OG. The R_L values between 0 and 1 confirmed that adsorption process is favourable for the entire concentration range under study because this parameter is continuously decreasing and is smaller than 1.

The applicability of the isotherm equations was estimated by R^2 values. The correlation coefficient value of 0.9927 indicates that this model describes very well the adsorption of OG on the A2 polymer at 298 K.

Table 4
Intraparticle diffusion parameters for the removal of OG dye at different initial dye concentrations

C_0 (mg L^{-1})	k_{id1} (mg g^{-1} $min^{-0.5}$)	I_{id1} (mg g^{-1})	R^2	k_{id2} (mg g^{-1} $min^{-0.5}$)	I_{id2} (mg g^{-1})	R^2
25	1.199	3.95	0.9502	–	–	–
50	2.679	9.38	0.9412	–	–	–
150	2.234	44.49	0.9406	–	–	–
250	8.036	54.34	0.9716	–	–	–
500	16.695	113.0	0.9859	1.128	230.3	0.9660
750	29.691	115.9	0.9987	4.988	305.9	0.9878

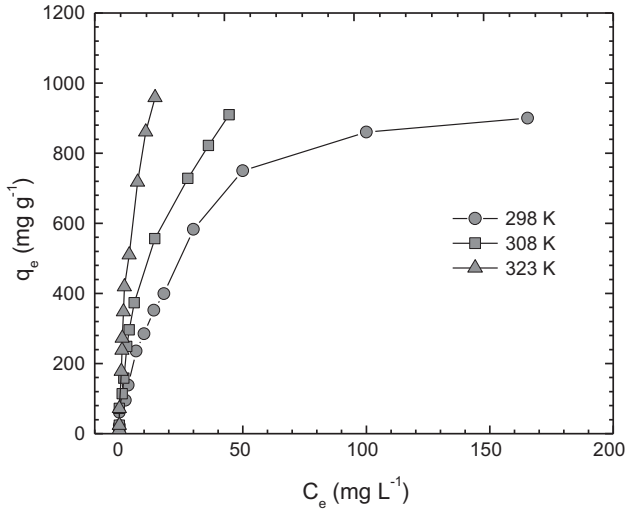

Fig. 6. Equilibrium isotherms for OG dye adsorption on A2 (pH 2; w = 0.05 g; V = 20 mL; 20 h).

The adsorbent has high adsorption capacity for the OG dye, comparable with that of EMCN [32] and much higher than other weak basic adsorbents with amine groups investigated in the literature (Table 7).

The K_F values indicate an increase of the adsorption capacity with increasing temperature which is in agreement with the results obtained using Langmuir model. The values of $1/n$ smaller than 1 (from 0.4115 to 0.5025) indicate favourable adsorption and a chemisorption process.

The adsorption data of the two-parameter models conforms as follows: Langmuir > Freundlich.

The R^2 values higher than 0.99 for the three-parameter isotherms revealed that these models fit the equilibrium data better when compared with two-parameter models.

Redlich–Peterson isotherm is a hybrid isotherm featuring both Langmuir and Freundlich isotherms, which incorporate three parameters into an empirical equation. The model is suitable to adsorption equilibria over a wide concentration range and can be applied either in homogeneous or heterogeneous systems due to its versatility [48]. When the value of β is equal to 1, the Redlich–Peterson equation is reduced to the Langmuir isotherm, while it reduced to a

Table 5
Non-linear forms of the tested isotherms and corresponding parameters

Isotherm	Non-linear form		Reference
Langmuir	$q_e = \frac{q_m b C_e}{1 + b C_e}$	q_m—maximum adsorption capacity of the adsorbent (mg g^{-1}) b—Langmuir constant related to the affinity of the binding sites (L mg^{-1})	[45]
Freundlich	$q_e = K_F C_e^{1/n}$	K_F—constant related to the adsorption capacity ((mg g^{-1})(mg L^{-1})$^{-1/n}$) n—Freundlich adsorption constant related to the adsorption intensity values	[45]
Redlich–Peterson	$q_e = \frac{K_{RP} C_e}{1 + a_{RP} C_e^{\beta}}$	K_{RP}—Redlich–Peterson constant (L g^{-1}) a_{RP}—Redlich–Peterson constant (L mg^{-1})$^{\beta}$ β—Redlich–Peterson exponent that lies between 0 and 1	[46]
Sips	$q_e = \frac{q_{mS} K_s C_e^{mS}}{1 + K_s C_e^{mS}}$	q_{mS}—maximum adsorption capacity of the adsorbent (mg g^{-1}) K_S—Sips constant related to the adsorption energy (L mg^{-1})^{mS} mS—Sips model exponent	[46]

Table 6
Isotherms parameters obtained using the non-linear method for the adsorption of OG onto A2 polymer at different temperatures

Isotherm	Parameter	Temperature		
		298 K	308 K	323 K
Langmuir	K_L (L g^{-1})	40.9	93.7	269.2
	q_m (mg g^{-1})	1,076	1,089	1,218
	b (L mg^{-1})	0.038	0.086	0.221
	R_L	0.51–0.01	0.32–0.005	0.15–0.002
	R^2	0.9927	0.9897	0.9879
Freundlich	K_F ($mg^{1-(1/n)}$ $L^{1/n}$ g^{-1})	122.9	143.7	257.2
	n	2.43	2.05	1.99
	R^2	0.9574	0.9913	0.9885
Redlich–Peterson	K_{RP} (L g^{-1})	38.9	167.2	425.6
	a_{RP} (L $mg^{-1})^{\beta}$	0.034	0.502	0.777
	β	1.00	0.71	0.73
	R^2	0.9919	0.9944	0.9913
Sips	q_{mS} (mg g^{-1})	1,042	1,761	1,882
	K_S (L $mg^{-1})^{mS}$	0.033	0.073	0.147
	mS	1.06	0.70	0.73
	R^2	0.9929	0.9937	0.9908

Freundlich isotherm, in case the value of the term $a_{RP}C_e$ is much higher than 1. The ratio of K_{RP}/a_{RP} indicates the adsorption capacity.

At 298 K, the Redlich–Peterson model reduces at Langmuir model since the exponent β equals unity. At higher temperatures, the β values of ~0.7 indicate that this model approaches the Langmuir model rather than the Freundlich model. An additional argument is the value of $a_{RP}C_e$ not higher than 1.

Sips isotherm is a combined form of Langmuir and Freundlich expressions deduced for predicting the heterogeneous adsorption systems. This hybrid model at low adsorbate concentrations reduces to Freundlich isotherm, while at high concentrations it predicts a monolayer adsorption capacity characteristic of the Langmuir isotherm. As a general rule, the equation parameters are governed mainly by the operating conditions such as the alteration of pH, temperature and concentration [48]. A good accordance between Redlich–Peterson, Sips and Langmuir maximum adsorption capacity was observed only at 298 K (K_{RP}/a_{RP} 1,144 mg g^{-1}, q_{mS} 1,042 mg g^{-1} and q_m 1,076 mg g^{-1}).

The experimental data have better fitted to Redlich–Peterson, Sips and Langmuir isotherm than to the other isotherm models tested.

3.4. Effects of adsorbent dosage

Fig. 7 presents the effect of adsorbent dosage on the percent dye removal and on q_e values. Due to A2 affinity for dye the percentage of OG removal is 97.8% for 0.02 g A2 and 100% for 0.25 g A2 (Fig. 7). These results can be attributed to the normal increase of the active surface area and of the number of adsorption sites available for adsorbent–dye interaction. Also, it can be observed that q_e decreased with the increase in the amount of the adsorbent. This may be attributed to the unsaturation of adsorption sites since the dose of polymer was increased at constant dye concentration [49].

The increase of adsorption up to a certain value with the adsorbent mass at constant concentration of dye was in general reported in the literature, but the shape of the obtained curves depends on the maximum adsorption capacity of the adsorbent tested. For adsorption of OG on PGME-deta, the dye removal percent sharply increased up to50 mg of sorbent mass (for initial dye concentration of 50 mg L^{-1}), and for masses higher than 110 mg, it gradually levelled off at 80% dye removal [25]. The percentage removal of OG with bagasse fly ash increased with the adsorbent dosage up to a certain limit and then it reached a constant value. Optimum adsorbent dosage for OG removal was 0.1 g per 50 mL of solution [8]. Adsorption of an anionic dye (eosin Y) from aqueous solution by TEPA–CS also increased with increasing adsorbent dosage and complete removal could be achieved at the dose of 500 mg L^{-1}. With increasing adsorbent dose, the quantity of dye adsorbed on the unit weight of the adsorbent gets reduced [31].

Table 7
Maximum capacity of OG dye adsorption for certain adsorbents with amine groups

q_m (mg g^{-1} or mmol g^{-1})	Adsorbent	Reference
123.9 mg g^{-1}	Poly(glycidyl methacrylate-*co*-ethylene glycol dimethacrylate) (PGME) functionalized with diethylene triamine (PGME-deta)	[25]
2.25 mmol g^{-1}	Ethylenediamine-modified magnetic chitosan nanoparticles	[32]
0.592 mmol g^{-1} (CAS)	Diethylenetriamine-modified native starch (CAS)	[34]
1.242 mmol g^{-1} (CAES)	Diethylenetriamine-modified enzymatic hydrolysed starch (CAES)	
0.591 mmol g^{-1}	Ethylenediamine modified starch	[33]
36.28 mg g^{-1} (298 K)	Amine-modified silica	[19]
40.12 mg g^{-1} (303 K)		
60.06 mg g^{-1} (313 K)		
48.98 mg g^{-1} (MAMPS)	Monoamine silica magnetite free (MAMMS)	[46]
61.33 mg g^{-1} (MAMMS)	Monoamine-modified magnetic silica (MAMMS)	
430 mg g^{-1}	Sawdusts bearing quaternary ammonium groups	[47]
4.35 mg g^{-1}	Untreated sawdusts	
1,076 mg g^{-1} (298 K)	Crosslinked acrylic copolymer functionalized with triethylenetetramine	In this paper
1,089 mg g^{-1} (308 K)		
1,218 mg g^{-1} (323 K)		

3.5. Effect of Na_2SO_4 on the adsorption capacity

The effect of Na_2SO_4 on the adsorption of OG dye was tested. In the absence of Na_2SO_4, at initial OG concentration of 400 mg L^{-1}, a dye percentage removal of 94.1% was reached. For Na_2SO_4 electrolyte concentrations from 2.5 to 7 g L^{-1}, the values of R (%) undergo an insignificant change from 94.5 to 93.5%, respectively. We should also mention that the electrolyte concentration is around 2.5 g L^{-1} in baths for dyeing with acid dyes [38].

In general, it is considered that inorganic anions of salts may compete for active sites on the adsorbent surface or deactivate the adsorbent [15]. A similar effect was observed for low concentration of electrolyte in the case of OG adsorption on mesoporous carbon. For the same system, the electrolyte in high concentrations has an opposite effect namely contributes to the reduction of the dye molecule dissociation and this effect causes the increase of dye adsorption on mesoporous adsorbent [9].

Adsorption on amine modified silica in the presence of NaCl increases for Acid Orange-12 dye while for OG dye decreases. This behaviour may be attributed to the different nature of interaction of the dyes with the adsorbent surface [19].

It is known that coloured wastewaters contain significant quantities of salts that may influence the dye

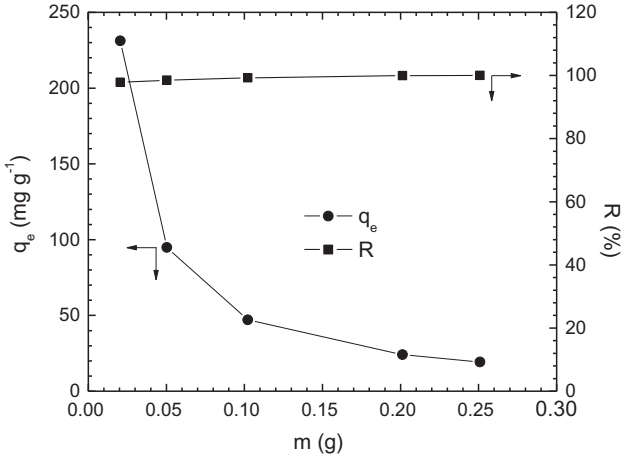

Fig. 7. Effect of A2 dosage on the percentage of dye removal and on amount of dye adsorbed at equilibrium (pH 2; 20°C; C_0 = 284 mg L^{-1}, V = 14 mL; 20 h).

Table 8
Thermodynamic parameters for the adsorption of OG on A2

Temperature (K)	KL (L g^{-1})	ΔG° (kJ mol^{-1})	$T\Delta S^\circ$ (kJ mol^{-1})	ΔH° (kJ mol^{-1})	ΔS° (J mol^{-1} K^{-1})
298	40.9	−9.23	69.42	60.19	232.97
308	93.7	−11.56	71.75		
323	269.2	−15.05	75.25		

removal. A reduced influence of electrolytes in dye removal from aqueous solutions suggests the possibility of adsorbent applying for textile wastewater containing salts.

3.6. Thermodynamics

The thermodynamic parameters ΔH° and ΔS°, namely enthalpy and entropy changes, respectively of the adsorption process can be evaluated by the van't Hoff equation using the values of K_L at different temperatures (Table 8) by the following relation (Eq. (5)) [45]:

$$\ln K_L = -\frac{\Delta H^\circ}{RT} + \frac{\Delta S^\circ}{R} \quad (5)$$

where ΔH°—adsorption enthalpy (kJ mol^{-1}); R—universal gas constant (J mol^{-1} K^{-1}); ΔS°—adsorption entropy (J mol^{-1} K^{-1}); T—temperature (K).

The dependence ln K_L vs. $1/T$ ($y = -7240.1x + 28.02$; $R^2 = 0.9995$), where the slope and intercept of the straight line are $\Delta H^\circ/R$ and $\Delta S^\circ/R$, respectively, gives the corresponding values for ΔH° and ΔS° (Table 8).

The positive value of ΔH° (60.19 kJ mol^{-1}) indicates that the adsorption is endothermic. Generally, the magnitude of the ΔH° value lies in the range of 2.1–20.9 kJ mol^{-1} and 80–200 kJ mol^{-1} for physical and chemical adsorption, respectively [50]. The ΔH° value of OG adsorption on A2 suggests involving other adsorption processes such as ion-exchange.

The positive value of ΔS° (232.97 J mol^{-1} K^{-1}) reflects an increased randomness at the solid–solution interface during adsorption of dye. From Table 8, it is observed that $|\Delta H^\circ| < |T\Delta S^\circ|$ and indicates that the adsorption process is driven by entropic rather than enthalpic changes [19].

The Gibbs-free energy of adsorption (ΔG°) was calculated from the following relation (Eq. (6)) and also is listed in Table 8.

$$\Delta G^\circ = \Delta H^\circ - T\Delta S^\circ \quad (6)$$

The negative values of ΔG° at all temperatures confirm the feasibility of the process and the spontaneous nature of OG adsorption onto the A2 polymer.

The ΔH° value for OG adsorption on amine modified silica of 28.56 kJ mol^{-1} has also been reported to be positive and is smaller than the values obtained in this study [19]. The favourable effect of temperature on dye adsorption is very important because most textile effluents are removed at relatively high temperature. For the EMCN [32] and monoamine-modified magnetic silica [46], the negative values of ΔH° indicate the exothermic nature of the process, due to structural characteristics of the adsorbents.

3.7. Characterization of polymer before and after dye adsorption

3.7.1. Scanning electron microscopy

The SEM micrographs show details on the modification of the morphological aspect of the polymer before and after dye adsorption. The functionalized polymer is characterized by certain microstructures with a system of cavities that differ in aspect and distribution. After dye adsorption, this morphological aspect is modified on both outer and inner surfaces (Fig. 8). It is evident that the surface becomes smooth due to the dye adsorbed and that a diffusion of the dye in pores occurred.

3.7.2. FT-IR spectra

The FT-IR spectrum (Fig. 9) of the A2 polymer shows the following characteristic bands: the doublet at 3,435–3,288 cm^{-1} and 3,412–3,267 cm^{-1}, specific for the absorption peak of NH_2 group; the bands at 2,924–2,929 cm^{-1} assigned to the asymmetrical and symmetrical stretching vibrations of CH_2 group; the characteristic peaks for the amide I ($\nu_{C=O}$ = 1,650–1,640 cm^{-1}) and amide II (ν_{N-H} = 1,560–1,551 cm^{-1}). After dye adsorption, the FT-IR spectrum of the A2-dye shows some important changes. There is a very intense band at 1,028 cm^{-1} assigned to the symmetrical stretching vibrations of SO_3 group coupled with the bands of medium intensity at 758 and 694 cm^{-1}.

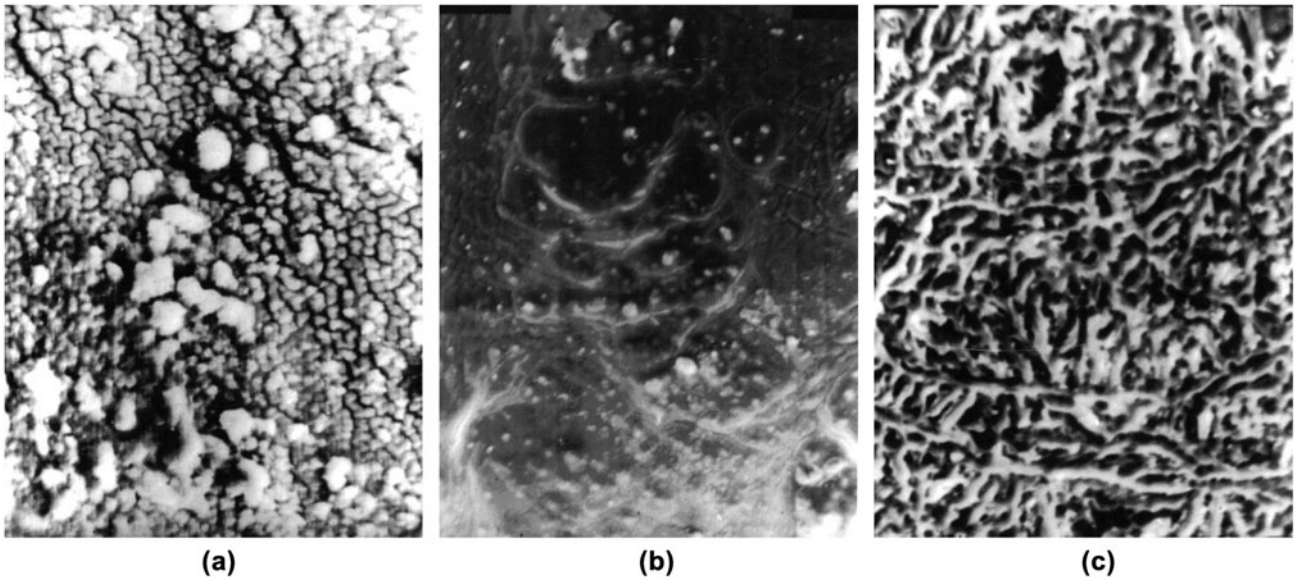

Fig. 8. SEM micrographs of functionalized polymer: (a) before OG adsorption and (b,c) after OG adsorption (×2000). (a) A2 surface; (b) A2 surface with OG dye; (c) A2 fracture with OG dye.

The band at 426 cm^{-1} corresponds to the wagging vibration mode of SO_3 group. The chromophore group (C–N=N–C) appears as an intense band at 1,003 cm^{-1}, and stretching vibration C–N of azo compound appears in IR spectrum at 1,207 cm^{-1} [51].

3.7.3. DTA and thermogravimetric analysis

A comparative analysis between the two samples based on the TG-DTG curves (Fig. 10(a)) allowed us to identify and separate three or four stages, respectively, of thermal degradation, and to evaluate the corresponding temperatures, weight losses and residue. Complex behaviour during thermal degradation, with three or more distinct stages, is reported in literature for functionalized polymers with N-containing groups [52]. Comparative analysis of the DTA curves (Fig. 10(b)) supports these findings.

As it can be seen from the DTG and DTA curves, as well as from the characteristic temperatures and weight losses, the first two stages of degradation are similar for the two samples. They are attributed to water loss and some low temperature polymer degradation. The greater weight loss and thermal effect in the first stage for the sample A2-OG indicates higher water content, due to the greater water affinity of the dye.

The A2 sample shows a complex degradation stage between 228 and 490˚C, leading to a total of 91% mass loss. This corresponds to stage IV in A2-OG degradation (Fig. 10(a)), with similar shape and characteristic temperatures between the two samples in both DTG and DTA curves. However, there is an additional process occurring during the polymer–dye composite degradation (major DTG peak at 307˚C), with considerable weight loss and thermal effect. This suggests a complex formation between the polymer and the dye, which breaks up at this temperature, as noted in literature for other polymer-dye composites [53]. The corresponding weight loss and the decrease of residue mass for A2-OG as compared to A2 lead to an estimate of around 30% ww of dye in the composite.

3.8. Column studies

The experimental results as obtained in adsorption columns of three different polymer bed heights (10, 20, and 30 mm) and flow rates (0.57, 0.87 and 1.13 mL min^{-1}) at an initial influent concentration (750 mg L^{-1}) and initial solution pH (2.0) were applied to the three mathematical models (Thomas, Yoon–Nelson and Wolborska) and the corresponding kinetic coefficients were determined using non-linear regression analysis. A brief description of these models is given hereafter.

Thomas model is one of the most general and widely used models in column performance theory. It is based on the assumption that the adsorption process follows Langmuir model of adsorption–desorption with no axial dispersion. The model

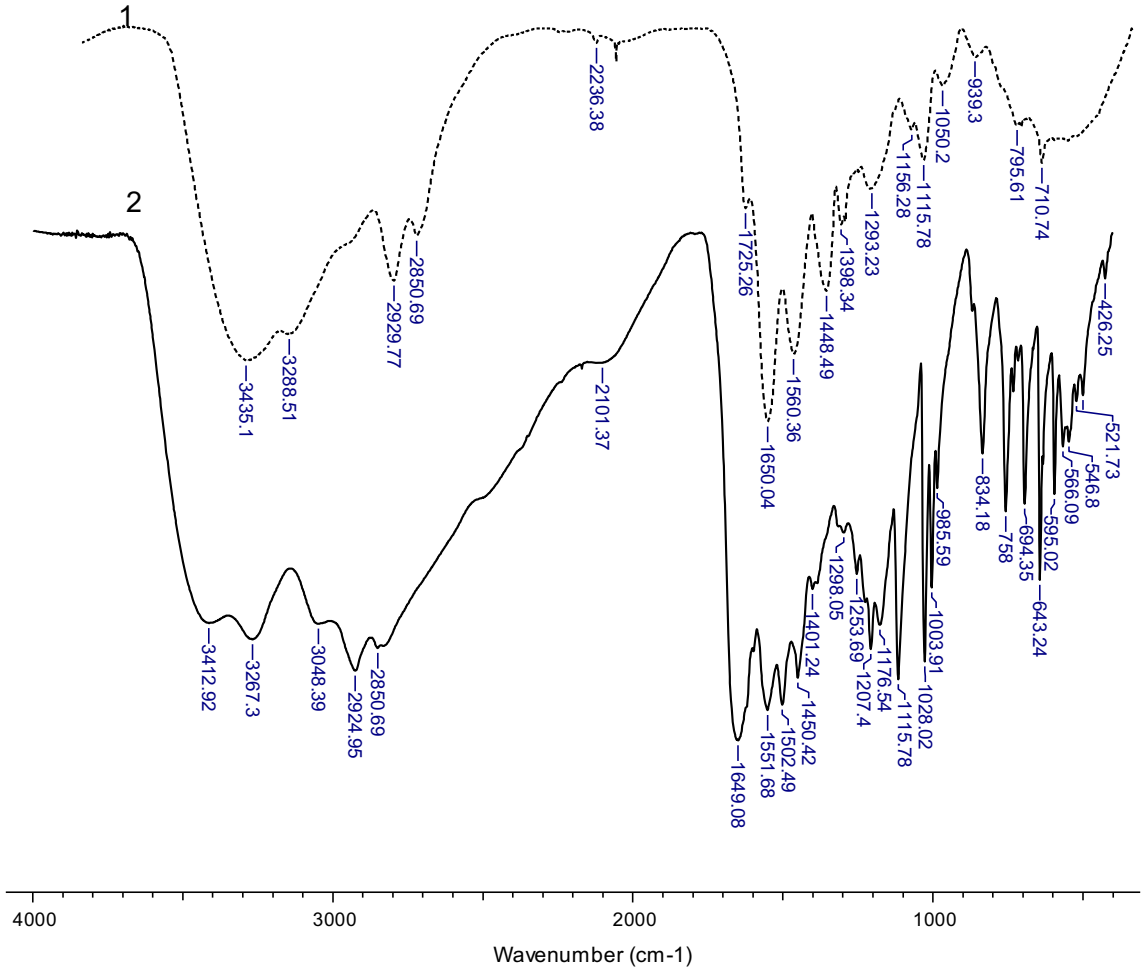

Fig. 9. FT-IR spectra: 1—A2 before OG adsorption; 2—A2 after OG adsorption.

behaviour matches with the pseudo-second-order reversible reaction kinetics [54]. The expression of Thomas model is given as follows (Eq. (7)):

$$\frac{C_t}{C_0} = \frac{1}{1 + \exp\left(\frac{k_T q_m m}{F} - \frac{k_T C_0}{F} V\right)} \tag{7}$$

where k_T is Thomas rate constant (L min^{-1} mg^{-1}), q_m is the maximum column adsorption capacity (mg g^{-1}), F is the flow rate of the effluent (L min^{-1}), m is the mass of the adsorbent (g) and V is the throughput volume (L).

Yoon–Nelson model is a relatively simple model for a single component system. It is based on the assumption that the rate of decrease in the probability of adsorption for each adsorbate molecule is proportional to the probability of adsorbate adsorption and the probability of adsorbate breakthrough on the adsorbent [54]. The following expression (Eq. (8)) represents the model:

$$\frac{C_t}{C_0} = \frac{\exp\left(k_{YN} t - t_{1/2} k_{YN}\right)}{1 + \exp\left(k_{YN} t - t_{1/2} k_{YN}\right)} \tag{8}$$

where k_{YN} is the rate constant (h^{-1}) and $t_{1/2}$ is the time required for 50% adsorbate breakthrough (h).

Wolborska model describes adsorption dynamics using mass-transfer phenomenon for the diffusion mechanism for low concentration range of breakthrough curves. The equation of the model (Eq. (9)) is represented as follows [54]:

$$\frac{C_t}{C_0} = \exp\left(\frac{\beta_a C_0}{N_0} t - \frac{\beta_a Z}{U_0}\right) \tag{9}$$

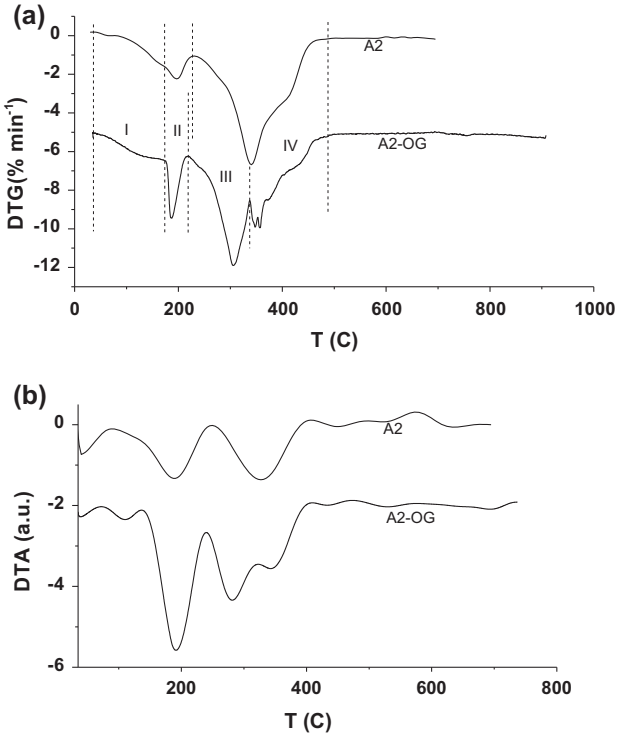

Fig. 10. DTG (a) and DTA (b) curves for thermal degradation of A2 and A2-OG.

where β_a is kinetic coefficient of external mass transfer (h^{-1}); N_0 is the bed capacity (mg L^{-1}); Z is the bed height (m); and U_0 is the linear flow rate (m h^{-1}).

The predicted and experimental breakthrough curves with respect to bed height and flow rate are shown in Fig. 11, while Table 9 illustrates the values of kinetic coefficients for each model used. To assess the prediction performance for each model, the values of R^2 are also depicted in Table 9. By comparing the R^2 values in Table 9 and superposition of experimental results and the predicted curves in Fig. 11, it is clear that the Thomas and Yoon–Nelson models adequately reproduce the experimental results for different bed heights and flow rates used. The rate constant k_T that characterizes the rate of solute transfer from the liquid to the solid phase increased with flow rate. The highest value indicates that the column adsorption is kinetically favourable.

The good fit of the experimental data to the Thomas and Yoon–Nelson models indicates that external and internal diffusion will not be the limiting step. Thomas and Yoon–Nelson models predict essentially the same uptake capacity for a particular experimental set of data as also suggested by Baral et al. [55] and Kushwaha and Sudhakar [56]. Wolborska model did not fit accurately the data from column experiments and a significant deviation between experimental and fitted data was observed ($R^2 < 0.80$). The values predicted by the Thomas model were closer to the Langmuir capacity (Table 9).

When Wolborska model was fitted to the full part of the breakthrough curves, a poor fit was obtained ($R^2 < 0.9$) for all the breakthrough curves (data not shown). Therefore, it was applied only to the initial part of the breakthrough curves (Table 9). The model was found valid only for predicting the initial part of the breakthrough curves (Fig. 11). The kinetic coefficient of the external mass transfer (β_a) decreased with increasing bed height and decreasing flow rate.

The flow rate is an important parameter affecting the breakthrough curves because it determines the contact period of the adsorbate with the adsorbent in the column. The breakthrough time and volume decreased with increasing influent flow rate (Fig. 11).

The time required for attaining the breakthrough or saturation, as well as the corresponding treated volume increased with increasing bed height. The column with greater bed height contains a larger amount of sorbent and thus provided a greater number of sites for the binding of metal ions, which resulted in a longer time for reaching breakthrough and saturation. Consequently, a larger volume of dye solution could be treated using higher bed height. Columns with short bed height were more quickly saturated due to lesser availability of adsorbent and hence the binding sites.

The maximum adsorption capacity estimated with Thomas and Yoon–Nelson models was higher at lower flow rates and longer bed heights.

3.9. Dye desorption

A suitable eluent must provide both efficiency of dye desorption and the preservation of adsorption capacity. The dye desorption occurs in basic medium as shown by the equation which is the reversion of the dye adsorption (Fig. 12)

In the presence of HO^- ions deprotonation of positively charged sites of polymer occurs which favours dye desorption and regeneration of A2 polymer. As seen in Fig. 13, the percentage of dye eluted in solution decreased from 99.5 to 36.3% with increasing concentration of NaOH solution from 0.01 to 0.5 mol L^{-1}. The most efficient eluent was NaOH solution 0.01 mol L^{-1} that quantitatively removes the adsorbed dye.

The adsorbent regenerated in column was washed with distilled water up to the neutral pH of the effluent. Then it was used in a new cycle of dye adsorption–desorption and it has been found that it

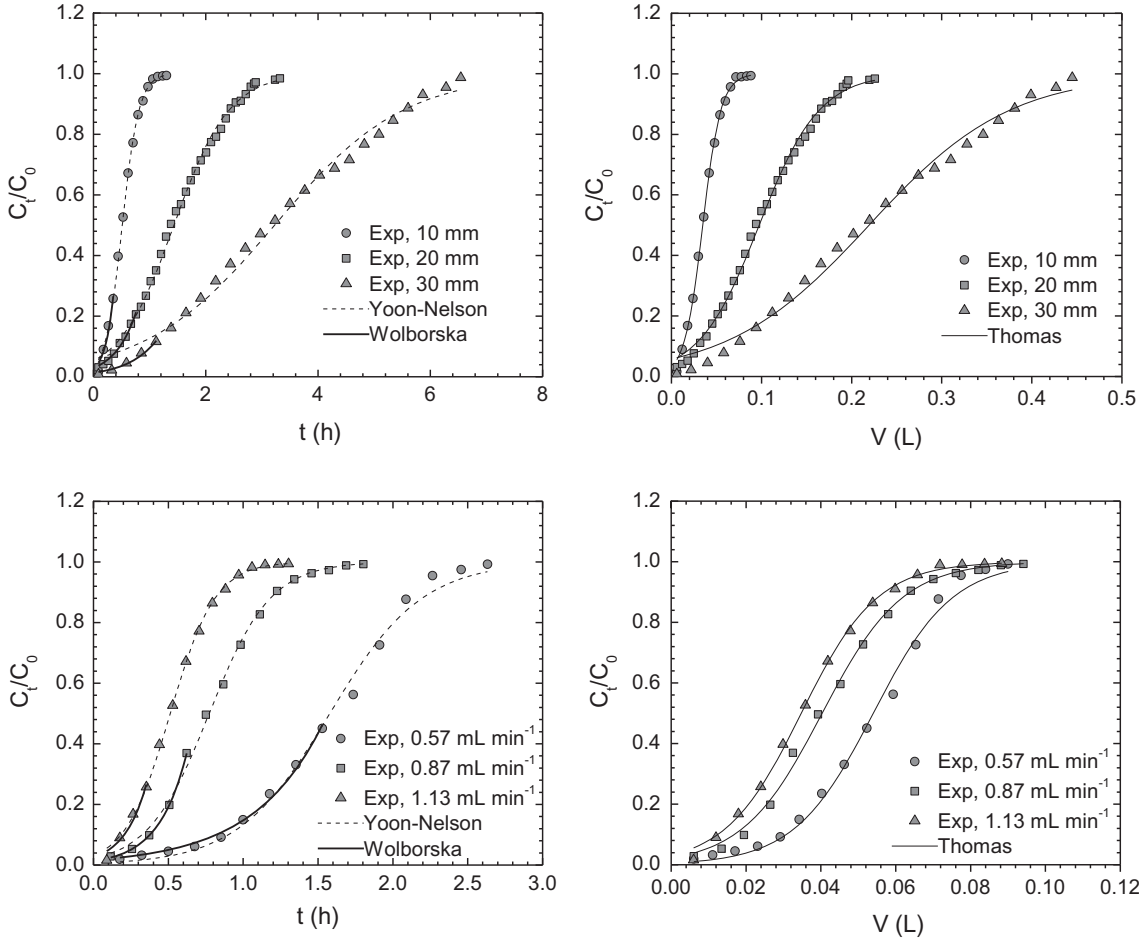

Fig. 11. Comparison of the predicted and experimental breakthrough curves obtained in adsorption columns at different bed heights and flow rates according to studied models for OG adsorption by A2.

Table 9
Model parameters obtained by nonlinear regression analysis for OG adsorption on A2

Experimental settings		Models									
		Thomas			Yoon–Nelson				Wolborska		
F (mL min^{-1})	Z (mm)	k_T (mL min^{-1} mg^{-1})	q_m (mg g^{-1})	R^2	k_{YN} (h^{-1})	$t_{1/2}$ (h)	q_m (mg g^{-1})	R^2	β_a (h^{-1})	q_m (mg g^{-1})	R^2
0.57	10	0.072	981	0.9944	3.24	1.58	981	0.9944	219	1,547	0.9936
0.87	10	0.109	765	0.9977	4.88	0.77	765	0.9976	354	1,016	0.9998
1.13	10	0.149	659	0.9987	6.67	0.51	659	0.9988	391	900	0.9564
1.13	20	0.045	917	0.9968	2.03	1.43	914	0.9969	189	1,094	0.9893
1.13	30	0.019	1,386	0.9911	0.87	3.23	1,382	0.9911	153	1,195	0.9818

had been fully recovered and the desorption ratio remained relatively constant (~99%). This behaviour is explained by the stability of the polymer in a wide pH range and so elution with diluted NaOH does not affect the structure of the polymer. Similarly, removal of the OG dye loaded onto amine-modified magnetic silica samples was carried out at pH 10 and a desorption per cent of 98% was obtained [46].

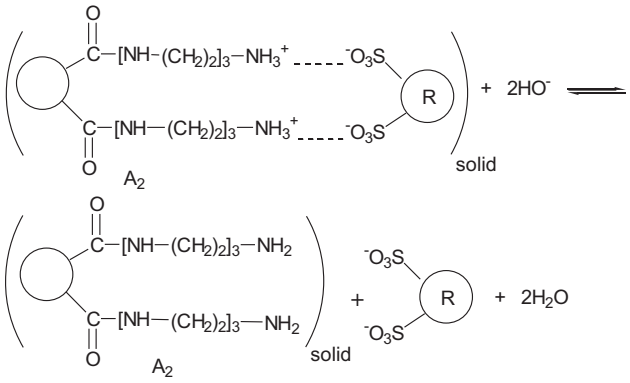

Fig. 12. Dye desorption in basic medium.

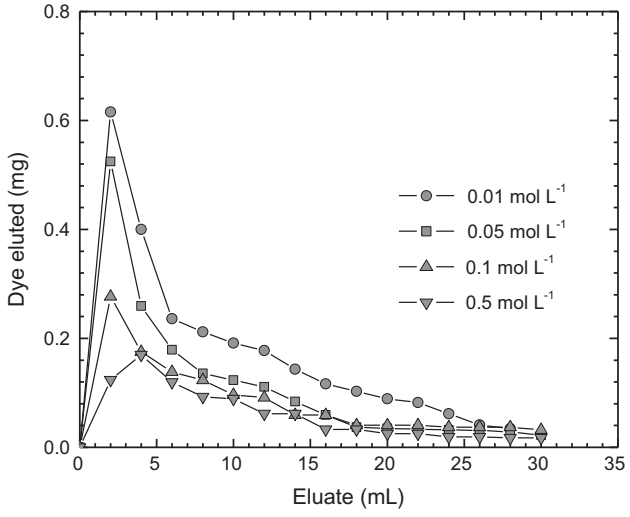

Fig. 13. The elution curves of OG dye with NaOH of various concentrations (0.05 g A2 loaded with 2.5 mg dye; rate flow of eluent 0.5 mL min^{-1}).

3.10. Adsorption mechanism

The results of testing different operational parameters related to OG dye adsorption on the polymer functionalized with TETA have shown that the adsorption mechanism is determined by the characteristics of the two participants, adsorbent and adsorbate. The high-adsorption capacity of the synthesized acrylic polymer investigated is explained by its morphological characteristics and surface chemical structure. Firstly, this resin has the property of swelling in water due to its low degree of crosslinking (2% DVB). The dry polymer forms gel structure after swelling and is characterized by porosity and a decreased density of amine groups. Secondly, TETA polyamine (with amino groups separated by ethylene moieties) used as functionalization agent of copolymer beads gives it long and flexible chain structure. At the same time, this long chain facilitates dye accessibility to amine groups of adsorbent reducing steric hindrance from closely agglomerated bulk gel particles. From the practice of separation, it is known that the materials functionalized with groups of large size and low density are well suited for the adsorption of high molecular weight compounds [57].

The adsorption mechanism is complex and ion exchange (electrostatic attractions) is suggested as the main one for adsorption of OG acid dye on the weak basic anion exchanger A2.

The polymer total exchange capacity of 14.66 mEg g^{-1} indicates a high affinity for the OG dye. This adsorbent has a high mean value of particle size (not higher than 300–800 μm) and a maximum adsorption capacity of 1,076 mg g^{-1} (at 298 K), comparable to that of EMCN (15–40 nm), of 1,050 mg g^{-1} at 293 K [32].

The most important parameter controlling the adsorption mechanism is the pH. Dye adsorption is optimum at pH 2.0 when protonation of free amino groups occurs, promoting interactions with the dye anions, correlated to the increasing of pH after adsorption. At pH values around 7, the ion exchange is probably not dominant. The almost complete desorption obtained with diluted NaOH also supports the ion exchange as the main adsorption process.

Kinetic studies have shown that intraparticle diffusion is not the rate-limiting step and the adsorption process is complex. These findings are supported by the good fit of the experimental data to Thomas and Yoon–Nelson models.

OG dye has a sulphonic salt structure that determines its solubility in water and dissociation in sulphonate anions. Along with dye dissociation, the dye spatial structure contributes to a high-adsorption capacity. Donia et al. [19] outlined that the optimized structure of OG indicates that minimum energy structures of the dye (with respect to amine-modified silica surface) assumes a twisted configuration. This twisted structure interacts basically through the two negatively charged sulphonate groups giving strong interaction with the available active sites of the adsorbent. Also, this kind of interaction gives no chance to H-bond formation.

4. Conclusions

The results obtained in the present study have shown that the synthesized A2 polymer based on crosslinked acrylic copolymer functionalized with TETA is a promising adsorbent for acid dye OG due to its high maximum adsorption capacity in the optimal conditions established (pH, contact time, dye concentration, adsorbent dose and temperature). The

adsorption data were fitted well by the Langmuir, Redlich–Peterson and Sips isotherm models. The maximum adsorption capacity at optimum pH 2 is dependent on temperature and was found to be 1,218 mg g^{-1} at 50°C. The adsorption process is endothermic and spontaneous in nature. The favorable effect of temperature on dye adsorption is very important because most textile effluents are removed at relatively high temperature. Of the three kinetic models applied, the pseudo-second-order model accurately described the adsorption kinetics at all concentrations studied. The electrostatic attraction between the dye anions and the protonated amine groups of the adsorbent plays an essential role for this system. Both surface and pore diffusion control the process in varying degrees depending on contact time and dye concentration. The presence of Na_2SO_4 electrolyte slightly affects adsorption and the dye can be efficiently removed with diluted NaOH solution. Thomas and Yoon–Nelson models successfully predicted breakthrough curves obtained for different bed heights and flow rates. The maximum adsorption capacity was higher at lower flow rates and longer bed heights.

Acknowledgements

This study is a contribution to the 730 CEEX Project funded by the Romanian Government.

References

[1] X. Zhou, X. Li, X. Chen, Binding mechanism of Orange G to human serum albumin: Saturation transfer difference-NMR, spectroscopic and computational techniques, Dyes Pigm. 98 (2013) 212–220.
[2] A. El-Ghenymy, F. Centellas, J.A. Garrido, R.M. Rodríguez, I. Sirés, P.L. Cabot, E. Brillas, Decolorization and mineralization of Orange G azo dye solutions by anodic oxidation with a boron-doped diamond anode in divided and undivided tank reactors, Electrochim. Acta 130 (2014) 568–576.
[3] M. Muthukumar, M.T. Karuppiah, G.B. Raju, Electrochemical removal of CI Acid orange 10 from aqueous solutions, Sep. Purif. Technol. 55 (2007) 198–205.
[4] M. Sharma, R.K. Vyas, K. Singh, A review on reactive adsorption for potential environmental applications, Adsorption 19 (2013) 161–188.
[5] M.T. Yagub, T.K. Sen, S. Afroze, H.M. Ang, Dye and its removal from aqueous solution by adsorption: A review, Adv. Colloid Interface Sci. 209 (2014) 172–184.
[6] Z. Aksu, A.I. Tatlı, Ö. Tunç, A comparative adsorption/biosorption study of Acid Blue 161: Effect of temperature on equilibrium and kinetic parameters, Chem. Eng. J. 142 (2008) 23–39.
[7] M. Arulkumar, P. Sathishkumar, T. Palvannan, Optimization of Orange G dye adsorption by activated carbon of Thespesia populnea pods using response surface methodology, J. Hazard. Mater. 186 (2011) 827–834.
[8] I.D. Mall, V.C. Srivastava, G.V.A. Kumar, I.M. Mishra, Characterization and utilization of mesoporous fertilizer plant waste carbon for adsorptive removal of dyes from aqueous solution, Colloids Surf., A 278 (2006) 175–187.
[9] A. Kaveh, G.A. Behdad, A.K. Amirhossein Haji, Equilibrium and kinetic adsorption study of the removal of Orange-G dye using carbon mesoporous material, J. Inorg. Mater. 27 (2012) 660–666.
[10] H. Tamai, T. Yoshida, M. Sasaki, H. Yasuda, Dye adsorption on mesoporous activated carbon fiber obtained from pitch containing yttrium complex, Carbon 37 (1999) 983–989.
[11] N. Bouchemal, Y. Azoudj, Z. Merzougui, F. Addoun, Adsorption modeling of Orange G dye on mesoporous activated carbon prepared from Algerian date pits using experimental designs, Desalin. Water Treat. 45 (2012) 284–290.
[12] C. Valderrama, J.L. Cortina, A. Farran, X. Gamisans, F.X. de las Heras, Kinetic study of acid red "dye" removal by activated carbon and hyper-cross-linked polymeric sorbents Macronet Hypersol MN200 and MN300, React. Funct. Polym. 68 (2008) 718–731.
[13] Y.M. Slokar, A. Majcen Le Marechal, Methods of decoloration of textile wastewaters, Dyes Pigm. 37 (1998) 335–356.
[14] S. Karcher, A. Kornmüller, M. Jekel, Screening of commercial sorbents for the removal of reactive dyes, Dyes Pigm. 51 (2001) 111–125.
[15] N.M. Mahmoodi, F. Najafi, A. Neshat, Poly (amidoamine-co-acrylic acid) copolymer: Synthesis, characterization and dye removal ability, Ind. Crops Prod. 42 (2013) 119–125.
[16] L. Chao, L. Zhaoyang, L. Aimin, L. Wei, J. Zhenmao, C. Jinlong, Z. Quanxing, Adsorption of reactive dyes onto polymeric adsorbents: Effect of pore structure and surface chemistry group of adsorbent on adsorptive properties, Sep. Purif. Technol. 44 (2005) 115–120.
[17] S. Drăgan, M. Cristea, A. Airinei, I. Poinescu, C. Luca, Sorption of aromatic compounds on macroporous anion exchangers based on polyacrylamide: Relation between structure and sorption behavior, J. Appl. Polym. Sci. 55 (1995) 421–430.
[18] F. Delval, G. Crini, S. Bertini, C. Filiatre, G. Torri, Preparation, characterization and sorption properties of crosslinked starch-based exchangers, Carbohydr. Polym. 60 (2005) 67–75.
[19] A.M. Donia, A.A. Atia, W.A. Al-amrani, A.M. El-Nahas, Effect of structural properties of acid dyes on their adsorption behaviour from aqueous solutions by amine modified silica, J. Hazard. Mater. 161 (2009) 1544–1550.
[20] M. Greluk, Z. Hubicki, Effect of basicity of anion exchangers and number and positions of sulfonic groups of acid dyes on dyes adsorption on macroporous anion exchangers with styrenic polymer matrix, Chem. Eng. J. 215–216 (2013) 731–739.
[21] M. Wawrzkiewicz, Z. Hubicki, Equilibrium and kinetic studies on the adsorption of acidic dye by the gel anion exchanger, J. Hazard. Mater. 172 (2009) 868–874.

[22] M. Wawrzkiewicz, Z. Hubicki, Kinetic studies of dyes sorption from aqueous solutions onto the strongly basic anion-exchanger Lewatit MonoPlus M-600, Chem. Eng. J. 150 (2009) 509–515.
[23] M. Wawrzkiewicz, Z. Hubicki, Weak base anion exchanger amberlite FPA51 as effective adsorbent for Acid Blue 74 removal from aqueous medium—kinetic and equilibrium studies, Sep. Sci. Technol. 45 (2010) 1076–1083.
[24] V. Dulman, C. Simion, A. Bârsănescu, I. Bunia, V. Neagu, Adsorption of anionic textile dye Acid Green 9 from aqueous solution onto weak or strong base anion exchangers, J. Appl. Polym. Sci. 113 (2009) 615–627.
[25] Z.P. Sandić, A.B. Nastasović, N.P. Jović-Jovičić, A.D. Milutinović-Nikolić, D.M. Jovanović, Sorption of textile dye from aqueous solution by macroporous amino-functionalized copolymer, J. Appl. Polym. Sci. 121 (2011) 234–242.
[26] H. Kaşgöz, Aminofunctionalized acrylamide-maleic acid hydrogels: Adsorption of indigo carmine, Colloids Surf., A 266 (2005) 44–50.
[27] H. Kaşgöz, New sorbent hydrogels for removal of acidic dyes and metal ions from aqueous solutions, Polym. Bull. 56 (2006) 517–528.
[28] L. Zhang, H. Wang, W. Yu, Z. Su, L. Chai, J. Li, Y. Shi, Facile and large-scale synthesis of functional poly(m-phenylenediamine) nanoparticles by Cu^{2+}-assisted method with superior ability for dye adsorption, J. Mater. Chem. 22 (2012) 18244–18251.
[29] J. Labanda, J. Sabaté, J. Llorens, Modeling of the dynamic adsorption of an anionic dye through ion-exchange membrane adsorber, J. Membr. Sci. 340 (2009) 234–240.
[30] J. Labanda, J. Sabaté, J. Llorens, Experimental and modeling study of the adsorption of single and binary dye solutions with an ion-exchange membrane adsorber, Chem. Eng. J. 166 (2011) 536–543.
[31] X.-Y. Huang, X.Y. Mao, H.T. Bu, X.Y. Yu, G.B. Jiang, M.H. Zeng, Chemical modification of chitosan by tetraethylenepentamine and adsorption study for anionic dye removal, Carbohydr. Res. 346 (2011) 1232–1240.
[32] L. Zhou, J. Jin, Z. Liu, X. Liang, C. Shang, Adsorption of acid dyes from aqueous solutions by the ethylenediamine-modified magnetic chitosan nanoparticles, J. Hazard. Mater. 185 (2011) 1045–1052.
[33] R. Cheng, S. Ou, M. Li, Y. Li, B. Xiang, Ethylenediamine modified starch as biosorbent for acid dyes, J. Hazard. Mater. 172 (2009) 1665–1670.
[34] Z. Wang, B. Xiang, R. Cheng, Y. Li, Behaviors and mechanism of acid dyes sorption onto diethylenetriamine-modified native and enzymatic hydrolysis starch, J. Hazard. Mater. 183 (2010) 224–232.
[35] R. Cheng, B. Xiang, Y. Li, M. Zhang, Application of dithiocarbamate-modified starch for dyes removal from aqueous solutions, J. Hazard. Mater. 188 (2011) 254–260.
[36] R. Cheng, S. Ou, B. Xiang, Y. Li, Q. Liao, Equilibrium and molecular mechanism of anionic dyes adsorption onto copper(II) complex of dithiocarbamate-modified starch, Langmuir 26 (2010) 752–758.
[37] R. Cheng, B. Xiang, Y. Li, Application of nickel(II) complex of dithiocarbamate-modified starch for anionic dyes removal from aqueous solutions, J. Appl. Polym. Sci. 123 (2012) 2439–2444.
[38] A. Bertea, V. Dulman, A.P. Bertea, I. Bunia, Recycle of polyamide dyeing wastewater following decolorization with polymeric sorbents, Environ. Eng. Manage J. 10 (2011) 305–310.
[39] R. Dhodapkar, N.N. Rao, S.P. Pande, T. Nandy, S. Devotta, Adsorption of cationic dyes on Jalshakti®, super absorbent polymer and photocatalytic regeneration of the adsorbent, React. Funct. Polym. 67 (2007) 540–548.
[40] Y.S. Ho, J.C.Y. Ng, G. McKay, Kinetics of pollutant sorption by biosorbents: Review, Sep. Purif. Methods 29 (2000) 189–232.
[41] S. Chowdhury, R. Mishra, P. Saha, P. Kushwaha, Adsorption thermodynamics, kinetics and isosteric heat of adsorption of malachite green onto chemically modified rice husk, Desalination 265 (2011) 159–168.
[42] N.A. Oladoja, A.K. Akinlabi, Congo red biosorption on palm kernel seed coat, Ind. Eng. Chem. Res. 48 (2009) 6188–6196.
[43] I.D. Mall, V.C. Srivastava, N.K. Agarwal, Removal of Orange-G and Methyl Violet dyes by adsorption onto bagasse fly ash: Kinetic study and equilibrium isotherm analyses, Dyes Pigm. 69 (2006) 210–223.
[44] G. Crini, P.M. Badot, Application of chitosan, a natural aminopolysaccharide, for dye removal from aqueous solutions by adsorption processes using batch studies: A review of recent literature, Prog. Polym. Sci. 33 (2008) 399–447.
[45] G. McKay, H.S. Blair, J.R. Gardner, Adsorption of dyes on chitin. I. Equilibrium studies, J. Appl. Polym. Sci. 27 (1982) 3043–3057.
[46] A.A. Atia, A.M. Donia, W.A. Al-Amrani, Adsorption/desorption behavior of acid orange 10 on magnetic silica modified with amine groups, Chem. Eng. J. 150 (2009) 55–62.
[47] V. Marchetti, P. Gerardin, B. Loubinoux, Preparation and use of sawdusts bearing quaternary ammonium groups for removal of anionic dyes from water, Holz Roh Werkst. 58 (2000) 53–56.
[48] K.Y. Foo, B.H. Hameed, Insights into the modeling of adsorption isotherm systems, Chem. Eng. J. 156 (2010) 2–10.
[49] A.E. Ofomaja, Y.S. Ho, Equilibrium sorption of anionic dye from aqueous solution by palm kernel fibre as sorbent, Dyes Pigm. 74 (2007) 60–66.
[50] F. Ji, C. Li, B. Tang, J. Xu, G. Lu, P. Liu, Preparation of cellulose acetate/zeolite composite fiber and its adsorption behavior for heavy metal ions in aqueous solution, Chem. Eng. J. 209 (2012) 325–333.
[51] K. Wojciechowski, S. Jerzy, Effect of the sulphonic group position on the properties of monoazo dyes, Dyes Pigm. 44 (2000) 137–147.
[52] J. Simitzis, E. Terlemesian, I. Mladenov, Utilization of waste PAN fibers as adsorbents by chemical and thermal modification, Eur. Polym. J. 31 (1995) 1261–1267.
[53] P.R. Somani, R. Marimuthu, A.K. Viswanath, S. Radhakrishnan, Thermal degradation properties of solid polymer electrolyte (poly(vinyl alcohol)+phosphoric acid)/methylene blue composites, Polym. Degrad. Stab. 79 (2003) 77–83.
[54] W. Zhang, L. Dong, H. Yan, H. Li, Z. Jiang, X. Kan, H. Yang, A. Li, R. Cheng, Removal of methylene blue

from aqueous solutions by straw based adsorbent in a fixed-bed column, Chem. Eng. J. 173 (2011) 429–436.
[55] S.S. Baral, N. Das, T.S. Ramulu, S.K. Sahoo, S.N. Das, G.R. Chaudhury, Removal of Cr(VI) by thermally activated weed Salvinia cucullata in a fixed-bed column, J. Hazard. Mater. 161 (2009) 1427–1435.
[56] S. Kushwaha, P.P. Sudhakar, Sorption of uranium from aqueous solutions using palm-shell-based adsorbents: A kinetic and equilibrium study, J. Environ. Radioact. 126 (2013) 115–124.
[57] D.C. Harris, Quantitative Chemical Analysis, W.H. Freeman and Company, New York, NY, 1982.